Title page

Calculation method of static carrying curve for double-row different-diameter ball slewing bearing

Yun-Feng Li, born in 1973, is currently a professor at *Henan University of Science and Technology, China*. He received his PhD degree from *Dalian University of Technology, China*, in 2006. His research interests include theoretical analysis and application of rolling bearing, mechanical system simulation, intelligent human-computer interaction.
Tel: +86-379-64231479; E-mail: liyunfeng@haust.edu.cn

Run-Dong Wang, born in 1987, is currently an engineer at *Luoyang Heavy-Duty Bearing Co., Ltd., China*. He received his master degree on mechanical engineering in *Henan University of Science and Technology*, *China*, in 2015.
E-mail: 1134964211@qq.com

Jin-Cheng Li, born in 1999, is currently a master candidate at *Henan University of Science and Technology, China*.
E-mail: 1098798693@qq.com

Corresponding author：Yun-Feng Li　E-mail：liyunfeng@haust.edu.cn

ORIGINAL ARTICLE

Calculation method of static carrying curve for double-row different-diameter ball slewing bearing

Yunfeng Li[1, 2] , Rundong Wang[3], Jincheng Li[1]

Received June xx, 201x; revised February xx, 201x; accepted March xx, 201x

Abstract: The calculation method of the static carrying curve of the double-row different-diameter ball slewing bearing was proposed. The relationship between the internal maximum rolling element load of each row and the external load combination of the slewing bearing was established by using the deformation compatibility conditions and the force equilibrium conditions. Using the rolling element load distribution range parameter of the main raceway and the auxiliary raceway of the double-row different-diameter ball slewing bearing respectively as input invariable, the corresponding external load combinations of axial load and tilting moment load of the slewing bearing were obtained. These external load combinations were plotted in the coordinate system to obtain the static carrying curve of the slewing bearing. The obtained static carrying curve was compared with that calculated by the finite element method for the verification purpose. Finally, influence laws of the detailed design parameters, such as raceway groove radius coefficient, raceway contact angle and rolling element diameter on the carrying capacity of the double-row different-diameter ball slewing bearing were analyzed by using the carrying curves. The results show that decreasing of raceway groove radius coefficient, increasing of rolling element diameter or increasing of raceway contact angle appropriately is advantageous for enhancing the carrying capacity of the double-row different-diameter ball slewing bearing.

Keywords: Slewing bearing, Carrying capacity, Mechanical model, Design parameter, Finite element analysis

✉ Yun-Feng Li
liyunfeng@haust.edu.cn

[1] School of Mechatronics Engineering, Henan University of Science and Technology, Luoyang 471003, China

[2] Collaborative Innovation Center of Machinery Equipment Advanced Manufacturing of Henan Province, Luoyang 471003, China

[3] Luoyang Heavy-Duty Bearing Co., Ltd. , Luoyang 471600, China

1 Introduction

Slewing bearings are key components of many mechanical systems, which are widely used in heavy machineries, such as crane, excavator, stacker, shield machine, etc. As a special rolling bearing with huge size and carrying combined heavy loads, it has attracted great attention of researchers in recent ten years. Some researchers paid attention to the modeling method of slewing bearing, and used the calculation model to analyze the factors affecting the load carrying performance. He et al. [1-2] investigated the effect of mesh size of the finite element model and the material parameters on the analysis of the maximum contact load, deformation, and load distribution of the single-row four-point contact ball slewing bearing. Zhang et al. [3] established the elastic mechanics based numerical models of a double-row four-point contact ball slewing bearing with the rigid rings and flexible rings respectively. The influences of the initial contact angle, the coefficient of groove curvature radius, the clearance on the maximum contact force were analyzed. Kania et al. [4] analyzed the contact phenomena in a single-row four-point contact ball slewing bearing that the increase in the contact angle may lead to the displacement of the contact zone towards the raceway edge. Raceway profile modification by introducing the transition curve was discussed for eliminating the pressure concentration at the raceway edge. Spiewak [5] proposed a two-stage analysis strategy of a double-row four-point ball slewing bearing which includes the analysis of the local ball-raceway contact and the analysis of the global load distribution for concerning the static carrying capacity. The calculations were performed by using the finite elements model. Yu et al. [6] studied the load distribution for a single-row four-point contact ball slewing bearing. The retainer force was considered for satisfying the force equilibrium of the balls. The result shows that the retainer reduces the number of contact balls in the slewing bearing, so the maximum

contact load increases compared to the situation when the retainer is not considered. Chen et al. [7] studied the effects of supporting structure and bolt connection on the fatigue life and carrying capacity of a double-row four-point contact ball slewing bearing by using finite element models. Potocnik et al. [8] presented a carrying capacity calculation method of a double-row four-point contact ball slewing bearing based on a vector description of the bearing geometry. The influence of multi-row geometry and predefined irregular geometry of the bearing on the contact load distribution was analyzed. Li and Jiang [9] proposed a method for checking the strength of a three-row roller slewing bearing by using the mixed finite element model. Both the structural strength of the rings and the contact strength of the raceway were analyzed. Li [10] analyzed the effects of the detailed design parameters such as axial clearance, contact angle, and roller semi-cone angle on the carrying capacity of a double-row tapered roller slewing bearing by solving a system of equilibrium equations. Gao et al. [11] studied the effect of raceway geometry parameters on the carrying capability and the service life of a single-row four-point contact ball slewing bearing by solving a set of non-linear equations.

Some researchers paid attention to the influence of machining error of slewing bearing on the load carrying capacity. Heras et al. [12,13]proposed a method for calculating the load distribution in a single-row four-point contact ball slewing bearing considering ball preload, manufacturing errors and ring flexibility. The mechanical model was built by the formulation and minimization of the potential energy of the bearing for considering the ring deformations. Aithal et al. [14] studied the influence of manufacturing errors on rolling element load distribution of a single-row four-point contact ball slewing bearing by using finite element method. It is observed that size error on the ball and waviness error on the raceway are the two influencing factors on load distribution. Starvin et al. [15] analyzed the effect of manufacturing tolerances on the load carrying capacity of large diameter ball bearings based on the finite element model. Monte Carlo simulation was used for allocating tolerance on balls and raceways.

While other researchers paid attention to the analysis, calculation and experimental test of slewing bearing. Liu et al. [16] built a finite element model for a slewing bearing to estimate the load distribution. Static loading experiment was performed by mounting strain gauges on the inside circumference of the inner ring to obtain load distribution. The comparison between numerical and experimental results was discussed. Chen et al. [17] proposed a method for measuring contact force in a single-row four-point contact ball slewing bearing. The deformation under the ball-raceway contact and the displacement of the end face of loaded bearing ring were measured. The ball-raceway contact force was determined by the finite element method based on the measured data. Hrcek et al. [18] established a finite element model of a single-row four-point contact ball slewing bearing for determining the axial stiffness characteristics. The axial stiffness was experimentally measured for verifying the results of finite element analysis. The mathematical expression of the deformation constant represented by the geometrical parameters, such as pitch diameters, rolling element diameters and contact angles was obtained by using a genetic algorithm.

Correct slewing bearing type selection is a prerequisite to ensure the safe and reliable application, while carrying capacity is an important indicator for the type selection of them. Slewing bearing mainly sustains the combined action of the axial load and the tilting moment load during operation, so the carrying capacity index of the slewing bearing should be able to show the ability to sustain the combined action of the axial load and the tilting moment load at the same time. The position of a point in two-dimensional coordinate space can represent two numbers composed of the axial load and the tilting moment load, therefore using a curve in two-dimensional coordinate system to represent the carrying capacity of the slewing bearing is a feasible method. The calculation of carrying curve of slewing bearing is a research hot spot in recent years. Aguirrebeitia et al. [19] presented a calculation method of acceptance surface of a single-row four-contact-point ball slewing bearing based on Sjovall and Rumbarger's equations. Aguirrebeitia et al. [20] established the geometrical interference model of a three-row roller slewing bearing. The calculation of acceptance curve in the load space was derived by using the model. Glodez et al. [21] established the static equilibrium equations of a single-row four-point contact ball slewing bearing by vector based approach. The static carrying capacity curve of the slewing bearing with and without clearance was calculated by solving the equations. Abasolo et al. [22] developed selection curves for a single-row four-point contact ball slewing bearing. The selection curves take into account the two possible static failure types, the ball-raceway contact failure and the bolted joint failure. Potocnik et al. [8] calculated the static carrying capacity curve of a double-row four-point contact ball slewing bearing considering irregular geometry. The effects of clearance and predefined irregular geometry of rings on the static capacity of the bearing were discussed. Li [23] calculated the static carrying capacity surface of a

double-row four-point contact ball slewing bearing by solving a system of equilibrium equations. The detailed design parameters, such as clearance, groove curvature and contact angle on the carrying capacity of the slewing bearing were analyzed. Aguirrebeitia et al. [24] developed a multi-parametric finite element model of a single-row four-point contact ball slewing bearing. Acceptance surface of the slewing bearing was calculated by using the model. Kania et al. [25][26] proposed a method of computing the carrying capacity of a slewing bearing based on the finite element model. The method considered the flexural-torsional flexibility of bearing rings, flexibility and number of clamping bolts.

The calculation methods of the carrying curve based on equilibrium equations[19-23] need the repeated numerical solution calculation which has much more computations. Although the finite element calculation method of the carrying curve [24-26] replaces the rolling elements with nonlinear truss elements for reducing the computing scale, a large number of iterative computations are needed to obtain the points composing the static carrying capacity curve.

The existing research works of carrying curve calculation are mainly in the theoretical stage, and the research results are not convenient to engineering application directly. The focus of this paper is to derive a calculation method of static carrying curve for slewing bearing with a simple and convenient calculating process for actual engineering application.

Double-row different-diameter ball slewing bearing is a commonly used structure form in practical engineering, as shown in Figure 1. It is composed of an inner ring, an outer ring, some rolling elements of main raceway and some rolling elements of auxiliary raceway. The rolling element of the main raceway which have a larger diameter mainly sustain the combined action of the axial load and the tilting moment load, while the rolling element of the auxiliary raceway which have a smaller diameter only sustain the action of the tilting moment load. This kind of slewing bearing has asymmetric up-down structure, and its mechanics modeling method is much more typical.

In this paper, the calculation method of the static carrying curve of the double-row different-diameter ball slewing bearing was derived, and the static carrying curve was calculated for a real case. The obtained carrying curve was compared with that calculated by the finite element method for the verification purpose. The main contributions of this paper are summarized as following:

1) The relationship between the maximum rolling element load of the main raceway and the maximum rolling element load of the auxiliary main raceway was established.

2) The external load combination of the axial load and the tilting moment load expressed by the maximum rolling element loads of the slewing bearing was derived.

3) A finite element model construction method for calculating the static carrying curve of the double-row different-diameter ball slewing bearing was proposed.

4) The sensitive factors affecting the carrying capacity of the double-row different-diameter ball slewing bearing were discovered.

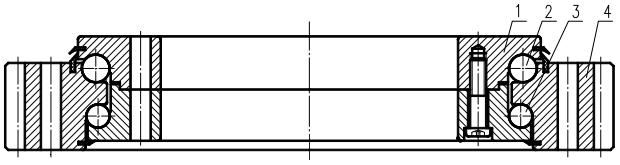

1-inner ring, 2-rolling element of main raceway, 3-rolling element of auxiliary raceway, 4-outer ring

Figure1 Structure of the double-row different-diameter ball slewing bearing

2 Mechanics Modeling

The static carrying capacity of the slewing bearing depends directly on the rolling element loads. They are the external load combinations that the slewing bearing can withstand as the maximum rolling element contact stress reaches the allowable contact stress of the raceway material. Therefore, the relationship between the external loads and the rolling element loads of the slewing bearing needed to be established. As external loads of the slewing bearing are given, the calculation of the rolling element load distribution belongs to the statically indeterminate problem. With the aid of deformation compatibility condition and force equilibrium condition, the mechanical model of the slewing bearing was established in this paper, and the relationship between the external loads and the rolling element loads was established further.

For the convenience of defining the position of each rolling element on the circumference of the slewing bearing, with the center of the slewing bearing as coordinate origin, establish a polar coordinate system in the radial plane of the slewing bearing. The polar axis of the coordinate system pass through the center of the most heavily loaded rolling element, and the angular position is represented by ψ. Then for each row of rolling elements, the angular position of each rolling element can be expressed as:

$$\psi = \frac{2\pi}{Z} i - \pi \tag{1}$$

where i is the sequence number of the rolling element,

($i = 1,2,\cdots,Z$), Z is the quantity of the rolling elements of main raceway or auxiliary raceway.

2.1 Deformation Compatibility Conditions

The outer ring of the slewing bearing is installed on the installation platform of the host machine and is fixed immovably, and the inner ring of the slewing bearing is combined with the rotating parts. The inner ring of the slewing bearing sustains the combined action of the axial load and the tilting moment load as the host machine being in operation. The inner ring of the slewing bearing produces displacements relative to the fixed outer ring under the action of the external loads. Suppose the corresponding axial displacement and angle displacement of the inner ring is δ_a and θ respectively under the combined action of external axial load F_a and tilting moment load M, as shown in Figure 2. Displacements of the inner ring bring about the contact loads between the rolling elements and the inner raceway and the outer raceway. The direction of the contact load Q_1 between the rolling element and the main raceways is represented as the contact direction 1, and the direction of the contact load Q_2 between the rolling element and the auxiliary raceways is represented as the contact direction 2. Let the indices 1 designates the contact direction 1, and 2 designates the contact direction 2 in the following.

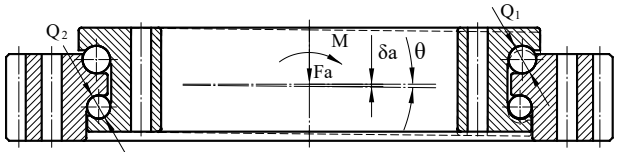

Figure2 Displacements of the inner ring under the combined load

Within a sufficiently small scope, the contact area between a rolling element and a raceway can be regarded as the contact of two parallel planes, as shown in Figure 3. For the contact direction 1, set the angular position of the most heavily loaded rolling element position as $\psi_1 = 0$, then the displacement along the axial direction at the contact center between the inner ring raceway and the rolling element caused by inner ring displacement at arbitrary angular position ψ_1 is:

$$\overline{AA'} = \delta_a + \frac{1}{2}\theta \cdot d_{m1} \cdot \cos\psi_1 \tag{2}$$

where d_{m1} is the distribution diameter of the rolling elements of the main raceway.

The total contact deformation along the normal direction of contact between the rolling element and the inner ring raceway and the outer ring raceway of contact direction 1 at arbitrary angular position ψ_1 is $\overline{AB}$, namely:

$$\delta_{\psi 1} = \left(\delta_a + \frac{1}{2}\theta \cdot d_{m1} \cdot \cos\psi_1 \right) \cdot \sin\alpha_1 \tag{3}$$

where α_1 is the contact angle between the rolling element and the main raceway.

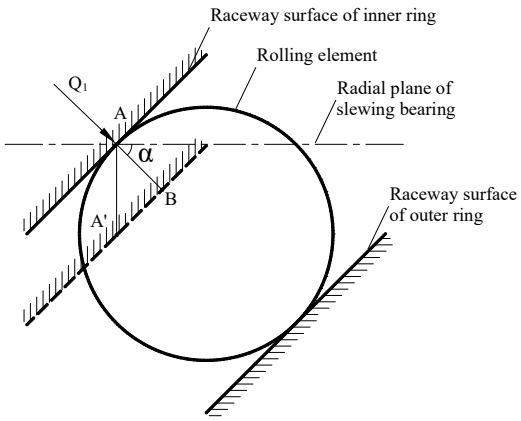

Figure3 Normal contact deformation

As can be seen from equation (3), the contact deformation at the angular position of $\psi_1 = 0$ is largest:

$$\delta_{\max 1} = \left(\delta_a + \frac{1}{2}\theta \cdot d_{m1} \right) \cdot \sin\alpha_1 \tag{4}$$

Define the rolling element load distribution range parameter of the main raceway as:

$$\varepsilon_1 = \frac{1}{2}\left(1 + \frac{2\delta_a}{\theta \cdot d_{m1}} \right) \tag{5}$$

Hence, from equation (3), (4) and (5), one can obtain the contact deformation at each angular position ψ_1:

$$\delta_{\psi 1} = \delta_{\max 1}\left[1 - \frac{1}{2\varepsilon_1}\left(1 - \cos\psi_1\right) \right] \tag{6}$$

According to Hertz contact theory, the relationship between the contact load Q and elastic deformation δ is [27]

$$Q = K_n \delta^{\frac{3}{2}} \tag{7}$$

where K_n is the total load-deformation constant between the rolling element and the inner ring raceway and the outer ring raceway.

By using equation (6) and (7), the rolling element load $Q_{\psi 1}$ at each angular position ψ_1 along the contact

direction 1 can be obtained as:

$$Q_{\psi 1}=Q_{\max 1}\left[1-\frac{1}{2\varepsilon_1}\left(1-\cos\psi_1\right)\right]^{\frac{3}{2}} \tag{8}$$

Similarly, the total contact deformation along the normal direction of the contact between the rolling element and the inner ring raceway and the outer ring raceway of contact direction 2 at each angular position ψ_2 is:

$$\delta_{\psi 2}=\left(-\delta_a+\frac{1}{2}\theta\cdot d_{m1}\cdot\cos\psi_2\right)\cdot\sin\alpha_2 \tag{9}$$

Obviously, the contact deformation of the contact direction 2 at the angular position of $\psi_2=\pi$ is largest, namely

$$\delta_{\max 2}=\left(-\delta_a+\frac{1}{2}\theta\cdot d_{m2}\right)\cdot\sin\alpha_2 \tag{10}$$

Define the rolling element load distribution range parameter of the auxiliary raceway as:

$$\varepsilon_2=\frac{1}{2}\left(1-\frac{2\delta_a}{\theta\cdot d_{m2}}\right) \tag{11}$$

Hence, from equation (9), (10) and (11), one can obtain the contact deformation at each angular position ψ_2:

$$\delta_{\psi 2}=\delta_{\max 2}\left[1-\frac{1}{2\varepsilon_2}\left(1-\cos\psi_1\right)\right] \tag{12}$$

The rolling element load $Q_{\psi 2}$ at each angular position angle ψ_2 along the contact direction 2 can be obtained as:

$$Q_{\psi 2}=Q_{\max 2}\left[1-\frac{1}{2\varepsilon_2}\left(1-\cos\psi_2\right)\right]^{\frac{3}{2}} \tag{13}$$

The following can be obtained by eliminating $\frac{2\delta_a}{\theta}$ in equation (5) and (11):

$$\varepsilon_2=\frac{1}{2}+\frac{d_{m1}}{d_{m2}}\left(\frac{1}{2}-\varepsilon_1\right) \tag{14}$$

Substitution of equation (4) and (10) into (7) yields

$$\frac{Q_{\max 1}}{Q_{\max 2}}=\frac{K_{n1}\delta_{\max 1}^{\frac{3}{2}}}{K_{n2}\delta_{\max 2}^{\frac{3}{2}}}=\frac{K_{n1}\left[\left(\delta_a+\frac{1}{2}\theta\cdot d_{m1}\right)\cdot\sin\alpha_1\right]^{\frac{3}{2}}}{K_{n2}\left[\left(-\delta_a+\frac{1}{2}\theta\cdot d_{m2}\right)\cdot\sin\alpha_2\right]^{\frac{3}{2}}} \tag{15}$$

Substitution of equation (5) and (11) into (15) yields

$$\frac{Q_{\max 1}}{Q_{\max 2}}=\frac{K_{n1}\left(\varepsilon_1\cdot d_{m1}\cdot\sin\alpha_1\right)^{\frac{3}{2}}}{K_{n2}\left(\varepsilon_2\cdot d_{m2}\cdot\sin\alpha_2\right)^{\frac{3}{2}}} \tag{16}$$

The following can be obtained further:

$$Q_{\max 1}=\frac{K_{n1}\left(\varepsilon_1\cdot d_{m1}\cdot\sin\alpha_1\right)^{\frac{3}{2}}}{K_{n2}\left(\varepsilon_2\cdot d_{m2}\cdot\sin\alpha_2\right)^{\frac{3}{2}}}Q_{\max 2} \tag{17}$$

$$Q_{\max 2}=\frac{K_{n2}\left(\varepsilon_2\cdot d_{m2}\cdot\sin\alpha_2\right)^{\frac{3}{2}}}{K_{n1}\left(\varepsilon_1\cdot d_{m1}\cdot\sin\alpha_1\right)^{\frac{3}{2}}}Q_{\max 1} \tag{18}$$

2.2 Force Equilibrium Conditions

According to equation (8) and (13), the inner ring sustains the action of all rolling element load $Q_{\psi 1}$ and $Q_{\psi 2}$ inside the slewing bearing, also sustains the action of external working loads F_a and M outside the slewing bearing. The inner ring is in equilibrium under the combined action of the internal loads and the external loads.

The equilibrium equation of axial load is

$$F_a=\sum_{\psi_1=-\pi}^{\psi_1=+\pi}Q_{\psi 1}\cdot\sin\alpha_1-\sum_{\psi_2=-\pi}^{\psi_2=+\pi}Q_{\psi 2}\cdot\sin\alpha_2 \tag{19}$$

The equilibrium equation of tilting moment is

$$M=\sum_{\psi_1=-\pi}^{\psi_1=+\pi}Q_{\psi 1}\cdot\sin\alpha_1\cdot\frac{1}{2}d_{m1}\cdot\cos\psi_1+\sum_{\psi_2=-\pi}^{\psi_2=+\pi}Q_{\psi 2}\cdot\sin\alpha_2\cdot\frac{1}{2}d_{m2}\cdot\cos\psi_2 \tag{20}$$

To facilitate calculation, the summation in the above two equations can also be written in integral form:

$$F_a = Z_1 \cdot Q_{\max 1} \cdot J_a(\varepsilon_1) \cdot \sin\alpha_1 - Z_2 \cdot Q_{\max 2} \cdot J_a(\varepsilon_2) \cdot \sin\alpha_2 \quad (21)$$

$$M = \frac{1}{2} d_{m1} \cdot Z_1 \cdot Q_{\max 1} \cdot J_m(\varepsilon_1) \cdot \sin\alpha_1 + \frac{1}{2} d_{m2} \cdot Z_2 \cdot Q_{\max 2} \cdot J_m(\varepsilon_2) \cdot \sin\alpha_2 \quad (22)$$

where

$$J_a(\varepsilon) = \frac{1}{2\pi} \int_{-\pi}^{+\pi} \left[1 - \frac{1}{2\varepsilon}(1 - \cos\psi) \right]^{\frac{3}{2}} d\psi \quad (23)$$

$$J_m(\varepsilon) = \frac{1}{2\pi} \int_{-\pi}^{+\pi} \left[1 - \frac{1}{2\varepsilon}(1 - \cos\psi) \right]^{\frac{3}{2}} \cos\psi d\psi \quad (24)$$

The relationship between the maximum rolling element loads $Q_{\max 1}$ and $Q_{\max 2}$ and the external loads F_a and M are established through equation (21) and (22).

2.3 Carrying Capacity Curve

If the restrictive values of $Q_{\max 1}$ and $Q_{\max 2}$ are given, taking values continuously for parameters ε_1 and ε_2 under the condition meeting equation (14), the static carrying curves of the main raceway and the auxiliary raceway will be obtained, as shown in the schematic diagram of Figure 4. The working loads F_a and M of the slewing bearing should satisfy the carrying capacity requirement of the main raceway and the auxiliary raceway simultaneously. That is they should fall within the shaded area of the diagram. So the carrying curve is composed of AB segment of the carrying curve of the auxiliary raceway and BC segment of the carrying curve of the main raceway. Therefore the coordinates of the intersection points A, B and C need to be determined firstly as plotting the static carrying curve.

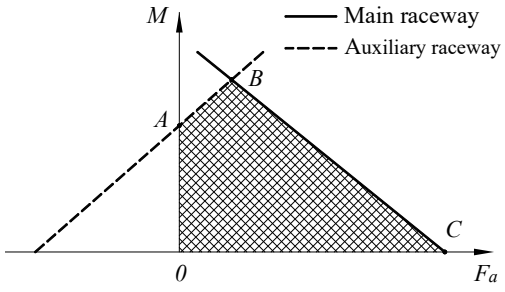

Figure4 Schematic diagram of the carrying curve

3 Calculation of Carrying Curve

3.1 Allowed Rolling Element Load

Slewing bearing usually works under the condition of overloading. This kind of working condition is easy to cause contact plastic deformation on the raceway surface. In order to avoid the influence of the plastic contact deformation of the raceway surface on the slewing performance, the total permanent deformation at the centre of the most heavily loaded rolling element-raceway contact should be limited to approximately 0.0001 of the rolling element diameter [28]. Double-row different-diameter ball slewing bearing adopts steel ball as rolling element. According to the experimental results of Qiu et al.[29], the allowable contact stress $[\sigma_{\max}]$ between the steel ball and the raceway surface of the slewing bearing made by the material of 42CrMo should be limited to 3600MPa. As calculating the static carrying curve, consider mainly the contact stress level between the most heavily loaded rolling element and the raceway surface. That is to calculate the various combinations of the axial load and the tilting moment load as the contact stress level between the most heavily loaded rolling element and the raceway equals to the limit value.

Hertz contact theory establishes the relationship between the contact load and the contact stress. For the point contact between the rolling element and the raceway surface, the maximum contact stress at the center of the contact area is:

$$\sigma_{\max} = \frac{1}{\pi n_a n_b} \left[\frac{3}{2} \left(\frac{\sum \rho}{\eta} \right)^2 Q \right]^{\frac{1}{3}} \quad (25)$$

where n_a and n_b is the dimensionless semimajor axis and the dimensionless semiminor axis of the contact ellipse respectively, η is the composite elastic constant of two elastic contact bodies, Q is the contact load. $\sum \rho$ is the curvature sum of two contact bodies. The curvature sum between the rolling element and the inner raceway can be expressed as the following:

$$\sum \rho_i = \frac{1}{D_w} \left(4 - \frac{1}{f_i} + \frac{2\gamma}{1-\gamma} \right) \quad (26)$$

where D_w is rolling element diameter, f_i is groove radius coefficient of inner raceway, $\gamma = \frac{D_w \cos\alpha}{d_m}$.

The curvature sum between the rolling element and the outer raceway can be expressed as the following:

$$\sum \rho_e = \frac{1}{D_w}\left(4-\frac{1}{f_e}+\frac{2\gamma}{1-\gamma}\right) \tag{27}$$

where f_e is groove radius coefficient of the outer raceway.

As the allowable contact stress $[\sigma_{\max}]$ at the contact center between the rolling element and the raceway surface is given, the allowable load of the most heavily loaded rolling element is:

$$[Q_{\max}] = \frac{2}{3}\left(\frac{\eta}{\sum \rho}\right)^2 (\pi m_a n_b [\sigma_{\max}])^3 \tag{28}$$

3.2 Calculation Procedure for Carrying Curve

Points on the static carrying curve should ensure that the main raceway and the auxiliary raceway all meet the requirements of the carrying capacity. So the allowable load $[Q_{\max 1}]$ of the most heavily loaded rolling element of the main raceway and the allowable load $[Q_{\max 2}]$ of the most heavily loaded rolling element of the auxiliary raceway should first be calculated out according to the equation (28). The calculation procedure of the carrying curve is as following:

Step 1: Calculate the intersection point of the static carrying curve of the auxiliary raceway and the vertical axis. As the load of the most heavily loaded rolling element of the auxiliary raceway equals to the allowable load $[Q_{\max 2}]$, the corresponding load $Q_{\max 1}$ of the most heavily loaded rolling element of the main raceway can be obtained by equation (17):

$$Q_{\max 1} = \frac{K_{n1}(\varepsilon_1 \cdot d_{m1} \cdot \sin\alpha_1)^{\frac{3}{2}}}{K_{n2}(\varepsilon_2 \cdot d_{m2} \cdot \sin\alpha_2)^{\frac{3}{2}}} \cdot [Q_{\max 2}] \tag{29}$$

Set $Q_{\max 2} = [Q_{\max 2}]$ and substitute equation (14) and (29) into equation (21) and (22), the following can be obtained:

$$F_a = Z_1 \cdot \frac{K_{n1}(\varepsilon_1 \cdot d_{m1} \cdot \sin\alpha_1)^{\frac{3}{2}}}{K_{n2}(\varepsilon_2 \cdot d_{m2} \cdot \sin\alpha_2)^{\frac{3}{2}}} \cdot [Q_{\max 2}] \cdot J_a(\varepsilon_1) \cdot \sin\alpha_1 - Z_2 \cdot [Q_{\max 2}] \cdot J_a\left[\frac{1}{2}+\frac{d_{m1}}{d_{m2}}\left(\frac{1}{2}-\varepsilon_1\right)\right] \cdot \sin\alpha_2 \tag{30}$$

$$M = \frac{1}{2} d_{m1} \cdot Z_1 \cdot \frac{K_{n1}(\varepsilon_1 \cdot d_{m1} \cdot \sin\alpha_1)^{\frac{3}{2}}}{K_{n2}(\varepsilon_2 \cdot d_{m2} \cdot \sin\alpha_2)^{\frac{3}{2}}} \cdot [Q_{\max 2}] \cdot J_m(\varepsilon_1) \cdot \sin\alpha_1 + \frac{1}{2} d_{m2} \cdot Z_2 \cdot [Q_{\max 2}] \cdot J_m\left[\frac{1}{2}+\frac{d_{m1}}{d_{m2}}\left(\frac{1}{2}-\varepsilon_1\right)\right] \cdot \sin\alpha_2 \tag{31}$$

Set $F_a = 0$, the value ε_{1A} of ε_1 corresponding to the intersection point A of the static carrying curve of the auxiliary raceway and the vertical axis can be obtained by the numerical solution of equation (30), and the value of M can be obtained by substituting ε_{1A} into equation (31) which is the vertical coordinate of the intersection point A of the carrying curve of the auxiliary raceway and the vertical axis.

Step 2: Calculate the intersection point of the static carrying curve of the auxiliary raceway and the static carrying curve of the main raceway. As the load of the most heavily loaded rolling element of the main raceway equals to the allowable load $[Q_{\max 1}]$, the corresponding load $Q_{\max 2}$ of the most heavily loaded rolling element of the auxiliary raceway can be obtained by equation (18):

$$Q_{\max 2} = \frac{K_{n2}(\varepsilon_2 \cdot d_{m2} \cdot \sin\alpha_2)^{\frac{3}{2}}}{K_{n1}(\varepsilon_1 \cdot d_{m1} \cdot \sin\alpha_1)^{\frac{3}{2}}} \cdot [Q_{\max 1}] \tag{32}$$

Set $Q_{\max 1} = [Q_{\max 1}]$ and substitute equation (14) and (32) into equation (21) and (22), the following can be obtained:

$$F_a = Z_1 [Q_{\max 1}] J_a(\varepsilon_1) \sin\alpha_1 - Z_2 \frac{K_{n2}(\varepsilon_2 \cdot d_{m2} \cdot \sin\alpha_2)^{\frac{3}{2}}}{K_{n1}(\varepsilon_1 \cdot d_{m1} \cdot \sin\alpha_1)^{\frac{3}{2}}} \cdot [Q_{\max 1}] \cdot J_a\left[\frac{1}{2}+\frac{d_{m1}}{d_{m2}}\left(\frac{1}{2}-\varepsilon_1\right)\right] \cdot \sin\alpha_2 \tag{33}$$

$$M = \frac{1}{2} d_{m1} \cdot Z_1 \cdot [Q_{\max 1}] \cdot J_m(\varepsilon_1) \cdot \sin\alpha_1 + \frac{1}{2} d_{m2} \cdot Z_2 \cdot \frac{K_{n2}(\varepsilon_2 \cdot d_{m2} \cdot \sin\alpha_2)^{\frac{3}{2}}}{K_{n1}(\varepsilon_1 \cdot d_{m1} \cdot \sin\alpha_1)^{\frac{3}{2}}} \cdot [Q_{\max 1}] \cdot J_m\left[\frac{1}{2}+\frac{d_{m1}}{d_{m2}}\left(\frac{1}{2}-\varepsilon_1\right)\right] \cdot \sin\alpha_2 \tag{34}$$

Let the right side of equation (30) be equal to the right side of equation (33), the value ε_{1B} of ε_1 corresponding to the intersection point B of the static carrying curve of the auxiliary raceway and the static carrying curve of the auxiliary raceway can be obtained

by the numerical solution. The value of F_a and M can be obtained by substituting ε_{1B} into equation (33) and (34) which is the coordinates of the intersection point B of the static carrying curve of the auxiliary raceway and the static carrying curve of the main raceway.

Step 3: Calculate the intersection point of the static carrying curve of the main raceway and the horizontal axis. Set $M=0$, the value ε_{1C} of ε_1 corresponding to the intersection point C of the static carrying curve of the main raceway and the horizontal axis can be obtained by the numerical solution of equation (34), the value of F_a can be obtained by substituting ε_{1C} into equation (33) which is the horizontal coordinate of the intersection point C of the carrying curve of the main raceway and the horizontal axis.

Step 4: Calculate the static carrying curve of the auxiliary raceway based on the carrying capacity of the auxiliary raceway. As ε_1 taking value in set $[\varepsilon_{1A},\varepsilon_{1B}]$ continuously and ε_2 taking value following ε_1 according to equation (14) , the corresponding values of F_a and M can be obtained by equation (30) and (31) which constitute the static carrying curve of the auxiliary raceway.

Step 5: Calculate the static carrying curve of the main raceway based on the carrying capacity of the auxiliary raceway. As ε_1 taking value in set $[\varepsilon_{1B},\varepsilon_{1C}]$ continuously and ε_2 taking value following ε_1 according to equation (14) , the corresponding values of F_a and M can be obtained by equation (33) and (34)which constitute the static carrying curve of the main raceway.

After completing the calculation of two segments of carrying curves AB and BC, smooth the region around the intersection point B , then the carrying curve of double-row different-diameter ball slewing bearing can be obtained.

4 Case Calculation

The proposed calculation method of the carrying curve of the double-row different-diameter ball slewing bearing was realized by using the Matlab programming environment. The parameters of a double-row different-diameter ball slewing bearing used in a shipyard crane are shown in Table.1. The coordinate data of the points on the static carrying curve were obtained by the calculation of the program. The static carrying curve diagram was plotted in the coordinate system by using the coordinate data.

Table1 Parameters of a slewing bearing

Parameter name		Value
Main raceway	D_{w1}/mm	45
	Z_1	173
	d_{m1}/mm	2990
	f_{i1}	0.525
	f_{e1}	0.525
	α_1/°	60
Auxiliary raceway	D_{w2}/mm	39.6875
	Z_2	196
	d_{m2}/mm	2980
	f_{i2}	0.525
	f_{e2}	0.525
	α_2/°	60

In order to verify the correctness of the established algorithm and calculation program in this paper, the results calculated by the algorithm were compared with those calculated by the commercial ANSYS finite element analysis software. In order to reduce the scale of finite element analysis, a mixed model composed of solid elements and spring elements was adopted for the finite element analysis of the double-row different-diameter ball slewing bearing assembly. The outer ring gear teeth which are irrelevant to the load carrying of the raceway were omitted. Detailed structures such as chamfer, sealing strip installation groove and so on were ignored. The rolling element was replaced by a nonlinear spring element COMBIN39, whose stiffness curve was calculated by equation (7). The rings were meshed by tetrahedral element SOLID92. All degree of freedom constraints were applied to the lower bottom surface of the outer ring. In order to facilitate the application of axial load and tilting moment load, a loading auxiliary node was established at the height center of the slewing bearing, which was meshed with the mass element MASS21, and then the auxiliary node is coupled with all nodes on the upper end face of the inner ring to form a rigid region. Finally, axial load and tilting moment load were applied on the auxiliary node. The scheme of the finite element model is shown in Figure 5. The geometric model and element model of the slewing bearing were established by using ANSYS software, as shown in Figure 6. The finite element model after applying the boundary conditions is shown in Figure 7.

Different combinations of axial load and tilting moment load were applied to the model in turn. When the calculated maximum rolling element load of the main

raceway reaches $[Q_{\max 1}]$ or the maximum rolling element load of the auxiliary raceway reaches $[Q_{\max 2}]$, a point on the carrying curve was obtained. The static carrying curve calculated by the finite element analysis software came into being by connecting all the neighboring plotted points.

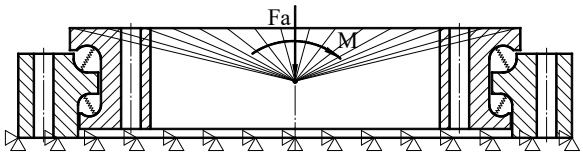

Figure5 Finite element modeling scheme

a) Geometric model b) Element model

Figure6 Models of slewing bearing

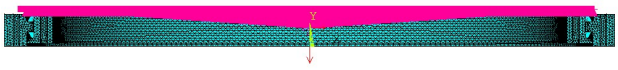

Figure7 Finite element model of slewing bearing

The static carrying curves calculated by the proposed method and the finite element method are shown in Figure 8. It can be seen from the figure that the curves obtained by the two methods are very close. The reason for the slight difference between the two is that the finite element method allows the structural deformation of the bearing rings.

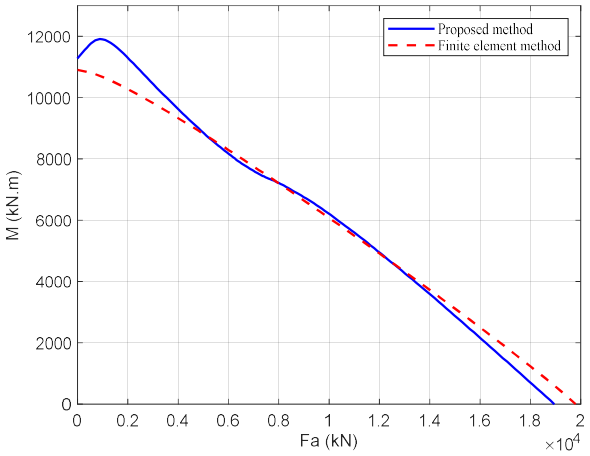

Figure8 Calculated carrying curve diagram

5 Analysis and Discussion

As the design parameters change, the load carrying capacity of the slewing bearing changes accordingly. So the position of the corresponding carrying curve in the coordinate system will change. In order to study the influence of the detailed design parameters on the static carrying capacity of double-row different-diameter ball slewing bearing, the raceway groove radius coefficient, rolling element diameter and raceway contact angle were taken different values respectively, and the corresponding static carrying curve was calculated.

The effect of raceway groove radius coefficient on the static carrying capacity of the double-row different-diameter ball slewing bearing is shown in Figure 9. As can be seen from the results in the figure, when the raceway groove radius coefficient increases from 0.515 to 0.530, the carrying capacity of the slewing bearing decreases accordingly. With the increase of the groove radius coefficient, the downward trend of the carrying capacity slows down. According to equation (28), the reduction of the raceway groove radius coefficient will increase the value of the allowable rolling element load $[Q_{\max}]$, so the allowable external loads F_a and M will increase accordingly. It can be seen that it is beneficial to improve the carrying capacity of the slewing bearing when the raceway groove radius coefficient is taken toward a small value.

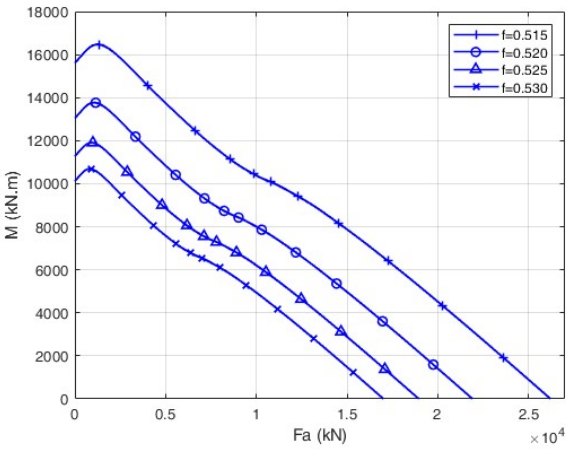

Figure9 Effect of groove radius coefficient

The effect of rolling element diameter on the static carrying capacity of the double-row different-diameter ball slewing bearing is shown in Figure 10. As can be seen from the results in the figure, when the rolling element diameter increases from 0.90 times the initial diameter to 1.05 times the initial diameter, the carrying capacity of the slewing

bearing increases accordingly. With the increase of the rolling element diameter, the rising trend of carrying capacity remains basically unchanged. According to equation (28), the increase of the rolling element diameter will increase the value of the allowable rolling element load $[Q_{\max}]$, so the allowable external loads F_a and M will increase accordingly. It can be seen that it is beneficial to improve the carrying capacity of the slewing bearing when the rolling element diameter is taken toward a large value.

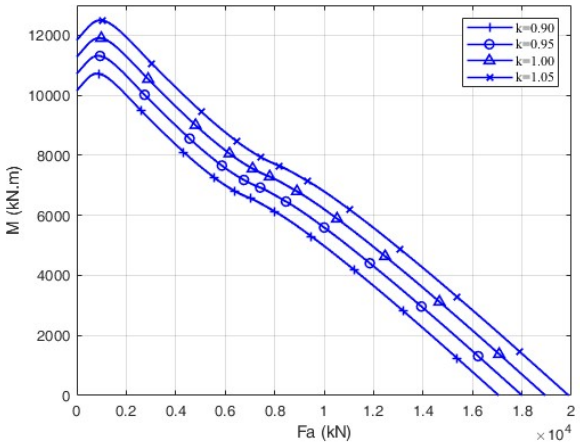

Figure10 Effect of rolling element diameter

The effect of contact angle on the static carrying capacity of the double-row different-diameter ball slewing bearing is shown in Figure 11. As can be seen from the results in the figure, when the contact angle increases from 50° to 65°, the carrying capacity of the slewing bearing increases accordingly. With the increase of the contact angle, the rising trend of carrying capacity remains basically unchanged. According to equation (19) and (20), the increase of the contact angle will increase the axial component $Q_\psi \cdot \sin\alpha$ of rolling element load increases, so the allowable external loads F_a and M will increase accordingly. It can be seen that it is beneficial to improve the carrying capacity of the slewing bearing when the contact angle is taken toward a large value.

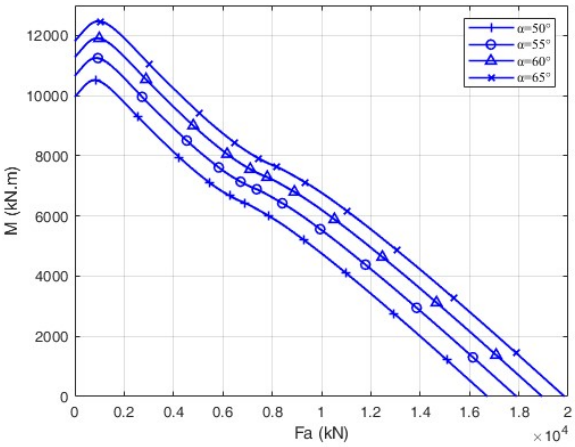

Figure11 Effect of raceway contact angle

6 Conclusions

Based on the statics modeling of double-row different-diameter ball slewing bearing, the calculation method of the static carrying curve was derived. Influence laws of the detailed design parameters on the carrying capacity of the double-row different-diameter ball slewing bearing were analyzed by using the static carrying curve. The following conclusions have been drawn:

(1) When the groove radius coefficient increases from 0.515 to 0.530, the carrying capacity of the slewing bearing decreases accordingly.

(2) When the rolling element diameter increases from 0.90 times the initial diameter to 1.05 times the initial diameter, the carrying capacity of the slewing bearing increases accordingly.

(3) When the contact angle increases from 50° to 65°, the carrying capacity of the slewing bearing increases accordingly.

Therefore decreasing of raceway groove radius coefficient, increasing of rolling element diameter or increasing of contact angle appropriately is advantageous for enhancing the carrying capacity of the double-row different-diameter ball slewing bearing.

7 Declaration

Funding

Supported by National Key R&D Program of China (Grant No. 2018YFB0407304) and Major Science and Technology Project of China National Machinery Industry Corporation (Grant No. SINOMAST-ZDZX-2019-02).

Availability of data and materials

The datasets supporting the conclusions of this article are

included within the article.

Authors' contributions

The author' contributions are as follows: Yunfeng Li was in charge of mechanics modeling and wrote the manuscript; Rundong Wang performed programming; Jincheng Li performed case calculation and data analyses.

Competing interests

The authors declare no competing financial interests.

Consent for publication

Not applicable

Ethics approval and consent to participate

Not applicable

References

[1] P Y He, Q R Qian, Y Wang, H Liu, E K Guo, H Wang. Influence of finite element mesh size on the carrying capacity analysis of single-row ball slewing bearing. *Advances in Mechanical Engineering*, 2021, 13(4): 1–12.

[2] P Y He, Y Wang, H Liu, E K Guo, H Wang. Influence of the elastic and elastic-plastic material parameters on the mechanical properties of slewing bearings. *Advances in Mechanical Engineering*, 2021, 13(1): 1–10.

[3] H W Zhang，S G Chen，Y T Dou，H M Fan，Y Q Wang. Mechanical model and contact properties of double row slewing ball bearing for wind turbine. *Reviews on Advanced Materials Science*, 2021, 60(1): 112–126.

[4] L Kania, R Pytlarz, S Spiewak. Modification of the raceway profile of a single-row ball slewing bearing. *Mechanism and Machine Theory*, 2018, 128: 1–15.

[5] S Spiewak. Methodology for calculating the complete static carrying capacity of twin slewing bearing. *Mechanism and Machine Theory*, 2016, 101: 181–194.

[6] Y H Yu, B R Lee, Y J Cho. New load distribution method for one-row slewing ball bearing considering retainer force. *International Journal of Precision Engineering and Manufacturing*, 2017, 18 (1): 49–56.

[7] G C Chen, C Z Wang, Z M Xiao. Effects of supporting structure and bolt connection on the fatigue life and carrying capacity of a slewing bearing. *Proceedings of the Institution of Mechanical Engineers, Part J: Journal of Engineering Tribology*, 2017, 231(6): 766–782.

[8] R Potocnik, P Goncz, S Glodez. Static capacity of a large double row slewing ball bearing with predefined irregular geometry. *Mechanism and Machine Theory*, 2013, 64: 67–79.

[9] Y F Li, D Jiang. Strength check of a three-row roller slewing bearing based on a mixed finite element model. *Proceedings of the Institution of Mechanical Engineers, Part C: Journal of Mechanical Engineering Science*, 2017, 231 (18): 3393–3400.

[10] Y F Li. Effects of design parameters on carrying capacity of a double-row tapered roller slewing bearing used in wind turbine. *Advances in Mechanical Engineering*, 2016, 8(7): 1–10.

[11] X H Gao, X D Huang, H Wang, R J Hong, J Chen. Effect of raceway geometry parameters on the carrying capability and the service life of a four-point-contact slewing bearing. *Journal of Mechanical Science and Technology*, 2010, 24 (10): 2083–2089.

[12] I Heras, J Aguirrebeitia, M Abasolo. Friction torque in four contact point slewing bearings: Effect of manufacturing errors and ring stiffness. *Mechanism and Machine Theory*, 2017, 112: 145–154.

[13] I Heras, J Aguirrebeitia, M Abasolo, I Coria, I Escanciano. Load distribution and friction torque in four-point contact slewing bearings considering manufacturing errors and ring flexibility. *Mechanism and Machine Theory*, 2019, 137: 23–36.

[14] S Aithal, Prasad N Siva, M Shunmugam, P Chellapandi. Effect of manufacturing errors on load distribution in large diameter slewing bearings of fast breeder reactor rotatable plugs. *Proceedings of the Institution of Mechanical Engineers, Part C: Journal of Mechanical Engineering Science*, 2016, 230(9): 1449–1460.

[15] M S Starvin, K Manisekar. The effect of manufacturing tolerances on the load carrying capacity of large diameter bearings. *Sadhana-Academy Proceedings in Engineering Sciences*, 2015, 40: 1899–1911.

[16] R Liu, H Wang, B T Pang, X H Gao, H Y Zong. Load distribution calculation of a four-point-contact slewing bearing and its experimental verification. *Experimental Techniques*, 2018, 42: 243–252.

[17] G C Chen, G Wen, Z M Xiao, H J San. Experimental study on contact force in a slewing bearing. *Journal of Tribology Transactions of the ASME*, 2018, 140 (2): 021402.1–021402.10.

[18] S Hrcek, R Kohar, J Steininger. Axial stiffness for large-scale ball slewing rings with four-point contact. *Bulletin of the Polish Academy of Sciences-Technical Sciences*, 2021, 69 (2): e136725.

[19] J Aguirrebeitia, R Aviles, I F de Bustos, M Abasolo. Calculation of general static load-carrying capacity for the design of four-contact-point slewing bearings. *Journal of Mechanical Design*, 2010, 132 (6): 064501.

[20] J Aguirrebeitia, M Abasolo, R Aviles, I F de Bustos. Theoretical calculation of general static load-carrying capacity for the design and selection of three row roller slewing bearings. *Mechanism and Machine Theory*, 2012, 48: 52–61.

[21] S Glodez, R Potocnik, J Flasker. Computational model for calculation of static capacity and lifetime of large slewing bearing's raceway. *Mechanism and Machine Theory*, 2012, 47: 16–30.

[22] M Abasolo, I Coria, J Plaza, J Aguirrebeitia. New selection curves for four contact point slewing bearings. *Proceedings of the Institution of Mechanical Engineers, Part C: Journal of Mechanical Engineering Science*, 2016, 230(10): 1715–1725.

[23] Y F Li. Analysis of influencing parameters on carrying capacity of pitch slewing bearing of wind turbine. *Acta Energiae Solaris Sinica*, 2018, 39: 3253–3260. (in Chinese)

[24] J Aguirrebeitia, M Abasolo, R Aviles, I F de Bustos. General static load-carrying capacity for the design and selection of four contact point slewing bearings: finite element calculations and theoretical model validation. *Finite Elements in Analysis and Design*, 2012, 55: 23–30.

[25] L Kania, M Krynke . Computation of the general carrying capacity of slewing bearings. *Engineering Computations*, 2013, 30(7): 1011-1028.

[26] L Kania, M Krynke, E Mazanek. A catalogue capacity of slewing

bearings. *Mechanism and Machine Theory*, 2012, 58: 29–45.
[27] T A Harris, M N Kotzalas. *Rolling Bearing Analysis: Essential Concepts of Bearing Technology*. 5th ed. Boca Raton: CRC Press, 2006.
[28] ISO 76: 2006. Rolling bearings - static load ratings.
[29] M Qiu, J F Yan, B H Zhao, P F Shi. Analysis of affecting factors on allowable contact stress of four-point-contact slewing rings with single row. *Key Engineering Materials*, 2012, 522: 260–263.

Biographical notes

Yun-Feng Li, born in 1973, is currently an professor at *Henan University of Science and Technology, China*. He received his PhD degree from *Dalian University of Technology, China*, in 2006. His research interests include theoretical analysis and application of rolling bearing, mechanical system simulation, intelligent human-computer interaction.
Tel: +86-379-64231479; E-mail: liyunfeng@haust.edu.cn

Run-Dong Wang, born in 1987, is currently an engineer at *Luoyang Heavy-Duty Bearing Co., Ltd., China*. He received his master degree on mechanical engineering in *Henan University of Science and Technology*, *China*, in 2015.
E-mail: 1134964211@qq.com

Jin-Cheng Li, born in 1999, is currently a master candidate at *Henan University of Science and Technology, China*.
E-mail: 1098798693@qq.com